

PACS numbers: 42.40.Eq; 42.65.An; 78.67.Bf; 82.70.Dd
DOI: 10.1070/QE2009v039n05ABEH013928

Degenerate two-wave mixing via a dynamic grating in Fe_3O_4 nanoparticle suspensions

E.Yu. Ageev, R.V. Litvinov, N.D. Khat'kov, L.V. Zagrebin, S.S. Shestov

Abstract. **Optical-gradient-force-induced spatially inhomogeneous disturbances of the dielectric permittivity of a suspension of spherical nanoparticles are analysed in the Maxwell Garnett approximation. Degenerate two-wave mixing in such media is shown to cause the formation of a spatial nanoparticle grating and the associated permittivity grating in the colloid. Relations are derived for the complex coupling constant of the waves. Codirectional and contradirectional two-wave mixing in suspensions of light-absorbing nanoparticles is considered. The two-beam coupling gain at 640 nm in various suspensions of Fe_3O_4 nanoparticles may reach ~ 10 cm^{-1}.**

Keywords: *optical nonlinearity, colloids, nanoparticles.*

1. Introduction

The optical nonlinearity of colloidal systems prepared from various dispersion media and solid nanoparticles as a dispersed phase manifests itself as a nonlinear and even nonmonotonic [1 – 4] dependence of their transmission on the incident intensity, self-focusing and defocusing of laser beams [3], degenerate optical phase conjugation [5] and the formation of spatial optical solitons [6, 7].

The nonlinear optical limiting and bleaching effects at 532 and 1060 nm in nanoparticles of wide-gap semiconductors and dielectrics (TiO_2, Al_2O_3, MgO, BaO and others) dispersed in VM-4 vacuum pump oil were attributed by Mikheeva and Sidorov [1] to photoconduction in a thin surface layer, which influenced the effective refractive index and extinction coefficient of the colloid. Kulchin et al. [3] reported optical nonlinearity of Al_2O_3 nanoparticle suspensions in VM-4 and immersion (cedarwood) oil at 633 and 532 nm: oscillations of their transmission as a function of incident intensity and light-induced axisymmetric changes in laser beam intensity, including the well-known self-focusing and defocusing effects [8 – 10]. They interpreted the observed nonlinear changes in the refractive index of the suspensions in terms of photoconduction in a thin surface layer of the nanoparticles (like in previous work [1]) and pointed out that the nonlinear response might be contributed by the temperature nonlinearity of the dispersion medium and quantum size effects.

Karavanskii et al. [2] used *z*-scan measurements at 532 nm (pulsed Nd : YAG laser, pulse width $\tau_p = 25$ ns) to assess the third-order nonlinearity of colloidal silver solutions prepared by laser ablation in water and ethanol. They showed that long-term (tens of hours) evolution of the colloids, due to aggregation and sedimentation processes, resulted in a transition from induced absorption to induced transparency, which was attributed to the formation of an oxide shell on the nanoparticles. Falcão-Filho et al. [4] recently studied the nonlinear optical response of aqueous suspensions of 10- to 30-nm-diameter silver nanoparticles to 80-ps Nd : YAG laser pulses. They used *z*-scan results to evaluate the nonlinearity of the refractive index and absorption coefficient of the suspensions up to the eighth order. At a fill factor (volume fraction of nanoparticles) $f = 1.47 \times 10^{-4}$, the Kerr coefficient n_2 of the colloid was determined to be -31×10^{-19} m^2 W^{-1}. The nonlinearity of the refractive index and absorption coefficient of the suspension was attributed to the nonlinear response of the constituent materials to a strong optical field far from resonance absorption lines [10]. At the same time, the observed nonlinear dependence of the changes in refractive index on f [4] suggests that there may be an additional mechanism of nonlinearity, e.g. the optical gradient force of the focused laser beam incident on the nanoparticles [11 – 14].

The optical nonlinearity of aqueous dispersions of polystyrene nanoparticles and air nanobubbles was modelled in terms of optical gradient forces [11 – 15], and the model was used to analyse spatial optical solitons [6, 7]. Gradient forces lead to a nonuniform nanoparticle distribution over the colloid and, as a consequence, give rise to spatially inhomogeneous disturbances of its dielectric permittivity [16, 17] and local inhomogeneities of light scattering [18 – 20].

Note that Matuszewski et al. [6] and El-Ganainy et al. [7] considered stationary soliton states developing in nanoparticle suspensions at high incident intensities (~ 10 GW m^{-2}), requiring sufficiently short pulse durations. The nonlinear response of a colloid can reach a steady-state level in time τ_p owing to the displacement of the nanoparticles under the action of the optical gradient force over a distance $L = \tau_p v$, which is of the same order as the diameter w_0 of the tightly focused light beam. Here, $v = qP$

E.Yu. Ageev, R.V. Litvinov, N.D. Khat'kov Tomsk State University of Control Systems and Radioelectronics, prosp. Lenina 40, 634050 Tomsk, Russia; e-mail: litvinovrv@rzi.tusur.ru;
L.V. Zagrebin, S.S. Shestov Centre for Information and Cell Medicine, Denisovskii per. 26/1, 105005 Moscow, Russia

Received 17 June 2008; revision received 2 September 2008
Kvantovaya Elektronika **39** (5) 435 – 441 (2009)
Translated by O.M. Tsarev

$\times d_p/(3\pi c\eta w_0^2)$ is the particle velocity [11]; q is the fraction of the light reflected from the particles; P is the incident power; c is the speed of light; and η is the viscosity of the liquid. Taking $P = 0.14$ GW; $\tau_p = 6$ ns; $q = 0.1$; $\eta = 1$ mPa s (water as the dispersion medium); $d_p = 50$ nm and $w_0 = 10$ μm, we obtain $L = 15$ μm. In the case of degenerate mixing of two or more waves in a colloidal system, the parameter that characterises the strong inhomogeneity of the intensity distribution is the period of the interference pattern Λ ($\Lambda \ll w_0$), with a power per period $\sim P\Lambda/w_0$. At $w_0 = 50$ μm and $\Lambda = 5$ μm, the displacement of a particle under the action of the optical gradient force resulting from the interference pattern is 6 μm. Thus, the optical nonlinearity of nanoparticle suspensions, due to optical gradient forces, can be used to bring about a variety of nonlinear optical effects.

In this paper, we analyse steady-state degenerate two-wave mixing via a dynamic holographic grating in a nanoparticle suspension.

2. Model

Consider the propagation of a monochromatic optical field of frequency ω in a suspension of spherical nanoparticles. The nanoparticle diameter d_p is considerably smaller than the wavelength of the light λ and than the skin layer thickness of the nanoparticle material. This allows light–suspension interaction to be analysed in the dipole approximation. In the absence of static electric and magnetic fields, the relative permittivity of the colloid, ε_c, can then be represented by the Maxwell Garnett formula [12–16]:

$$\varepsilon_c = \varepsilon_b + 3NV_p \frac{\varepsilon_b(\varepsilon_p - \varepsilon_b)}{\varepsilon_p + 2\varepsilon_b - NV_p(\varepsilon_p - \varepsilon_b)}, \quad (1)$$

where ε_b and ε_p are the relative permittivities of the dispersion medium and dispersed phase, respectively, at the frequency of the light wave; and N and $V_p = \pi d_p^3/6$ are the nanoparticle concentration and volume, respectively. The NV_p product is the volume fraction of nanoparticles, or fill factor f. In colloids $f \ll 1$ and, in the general case of light-absorbing dispersion media with nonlinear optical properties, one can neglect the contribution to the permittivity of the colloid, ε_c, from the small corrections $|\Delta\varepsilon_b| \ll |\varepsilon_b|$ and $|\Delta\varepsilon_p| \ll |\varepsilon_p|$ to the permittivities of its components, ε_b and ε_p, which appear in the second term on the right-hand side of Eqn (1). Below, we consider colloids with nonabsorbing dispersion media that have linear optical properties. The expression for ε_c then takes the form

$$\varepsilon_c = n_b^2 + 3NV_p n_b^2 \frac{\varepsilon_p' - i\varepsilon_p'' - n_b^2}{\varepsilon_p' - i\varepsilon_p'' + 2n_b^2}, \quad (2)$$

where n_b is the refractive index of the dispersion medium, and ε_p' and ε_p'' are, respectively, the real and imaginary parts of the permittivity of the dispersed phase.

The optical field exerts a gradient force $\boldsymbol{F}$ on the nanoparticles [10–15]. In the case of a monochromatic optical field propagating in a nonmagnetic medium, the gradient force can be represented as

$$\boldsymbol{F} = \frac{\alpha}{2}\nabla(\boldsymbol{E}\boldsymbol{E}^*), \quad (3)$$

where $\nabla = (\partial/\partial x)\boldsymbol{e}_x + (\partial/\partial y)\boldsymbol{e}_y + (\partial/\partial z)\boldsymbol{e}_z$; $\boldsymbol{e}_x$, $\boldsymbol{e}_y$ and $\boldsymbol{e}_z$ are the Cartesian unit vectors; and $\boldsymbol{E}$ is the electric vector of the optical field. Polarisation of a spherical particle at the frequency of the optical field can be represented as [18–20]

$$\alpha = 3V_p\varepsilon_0 n_b^2 \frac{\varepsilon_p' - i\varepsilon_p'' - n_b^2}{\varepsilon_p' - i\varepsilon_p'' + 2n_b^2}, \quad (4)$$

where ε_0 is the permittivity of vacuum.

Like in previous studies concerned with analysis of spatial solitons in nanoparticle suspensions [6, 7], we consider a steady-state self-action of the optical field in a colloid. The nanoparticle flux $\boldsymbol{j}$ produced by the gradient force $\boldsymbol{F}$ meets the equation [21, 22]

$$\nabla\boldsymbol{j} = \nabla(\mu N\boldsymbol{F} - D\nabla N) = 0, \quad (5)$$

where μ is the mobility of the particles, which can be expressed through their diffusion coefficient using the Einstein relation: $D = k_B T\mu$ (here, k_B is the Boltzmann constant and T is the absolute temperature).

The light-induced local changes of the nanoparticle concentration N in the colloid give rise to spatially inhomogeneous disturbances of its permittivity [see Eqn (2)], which in turn influence the optical field. Another mechanism that influences the optical field in the colloid is Rayleigh scattering from nanoparticles [18–20]. The local energy losses of the optical field through Rayleigh scattering can be quantified by the coefficient $\alpha_{sc} = N\sigma_{sc}$ (where σ_{sc} is the effective scattering cross section), which can be represented in the case under consideration as

$$\alpha_{sc} = \frac{2}{3}N\pi^5 n_b^4 \frac{d_p^6}{\lambda^4} \frac{(\varepsilon_p' - n_b^2)^2 + \varepsilon_p''^2}{(\varepsilon_p' + 2n_b^2)^2 + \varepsilon_p''^2}. \quad (6)$$

In general, as a result of the heating of the colloid through light absorption by the nanoparticles and dispersion medium, the temperature nonlinearity of the medium influences the optical field [3, 10, 23]. However, estimates made by Karpov et al. [23] in studies of the optical nonlinearity of hydrosols containing silver nanoparticles show that the thermal mechanism makes no significant contribution to the nonlinear response of the medium to 15-ns light pulses of intensity 8 GW cm^{-2}. Therefore, in what follows we neglect the thermal component of the nonlinear response.

The Helmholtz equation for the electric vector of the optical field,

$$\nabla^2\boldsymbol{E} + (k^2\varepsilon_c - i\alpha_{sc}n_b k)\boldsymbol{E} = 0 \quad (7)$$

(where k is the wavenumber), and Eqns (2)–(6) describe steady-state dynamic light scattering in a nanoparticle suspension, with allowance for optical-field absorption and scattering.

3. Wave mixing via a dynamic grating

Consider degenerate wave mixing in a colloid for the fields

$$\boldsymbol{E}_R = \boldsymbol{R}\exp[i(\omega t - \boldsymbol{k}_R\boldsymbol{r})], \text{ and } \boldsymbol{E}_S = \boldsymbol{S}\exp[i(\omega t - \boldsymbol{k}_S\boldsymbol{r})] \quad (8)$$

of the reference and signal beams, respectively, in transmission (Fig. 1a) and reflection (Fig. 1b) geometries. Like in previous studies [6, 7], the colloid is situated in a vessel whose dimensions considerably exceed the beam diameter. Far away from the beam axis, the nanoparticle flux is then zero ($\boldsymbol{j}(x, z \to \pm\infty) = 0$), and the nanoparticle concentration N_0 is equal to that in the dark. From Eqns (3) and (5), one can derive a relation between concentration N and the electric vector $\boldsymbol{E}$ of the optical field under these conditions:

$$N = N_0 \exp\left(\frac{\alpha}{4k_B T}\boldsymbol{E}\boldsymbol{E}^*\right) \approx N_0\left(1 + \frac{\alpha}{4k_B T}\boldsymbol{E}\boldsymbol{E}^*\right). \quad (9)$$

At an incident intensity of ~ 1 GW m^{-2} and a refractive index of the colloid close to that of water, $n_b = 1.33$, the absolute square of the electric vector of the optical field, $J = \boldsymbol{E}\boldsymbol{E}^*$, is $\sim 10^{11}$ V^2 m^{-2}. At a nanoparticle concentration of $\sim 10^{20}$ m^3 and nanoparticle diameter of ~ 100 nm, the exponent in (9) is much less than unity, and the Taylor series expansion of the exponential can be restricted to the linear term.

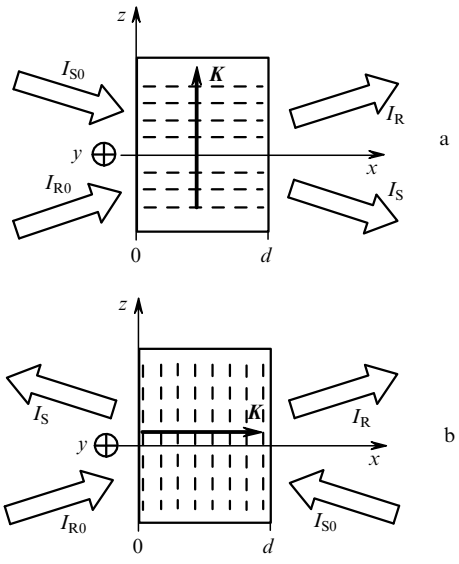

Figure 1. (a) Codirectional and (b) contradirectional two-wave mixing configurations in a nonlinear medium ($\boldsymbol{K} = \boldsymbol{k}_R - \boldsymbol{k}_S$).

The total electric field $\boldsymbol{E} = \boldsymbol{E}_R + \boldsymbol{E}_S$ produces a spatial grating of nanoparticles with a concentration

$$N \approx N_0 + \left[\frac{\alpha N_0 \boldsymbol{S}\boldsymbol{R}^*}{4k_B T}\exp(\boldsymbol{K}\boldsymbol{r}) + \text{c. c.}\right], \quad (10)$$

where $\boldsymbol{K} = \boldsymbol{k}_R - \boldsymbol{k}_S$. The grating gives rise to spatially inhomogeneous disturbances of the permittivity of the colloid and light scattering [see (2), (6) and (7)], leading to variations in the wave amplitudes $\boldsymbol{E}_R$ and $\boldsymbol{E}_S$ along the coupling length, which are slow compared to those over the wavelength. Using the method of slowly varying amplitude to solve Helmholtz equation (7), we can obtain equations for the coupled waves in the paraxial approximation:

$$\frac{d\boldsymbol{S}}{dx} = \mp i\frac{H}{2}(\boldsymbol{S}\boldsymbol{R}^*)\boldsymbol{R}, \quad \frac{d\boldsymbol{R}}{dx} = -i\frac{H^*}{2}(\boldsymbol{S}^*\boldsymbol{R})\boldsymbol{S}, \quad (11)$$

where the minus sign in the former equation corresponds to codirectional propagation (Fig. 1a), and the plus sign, to contradirectional propagation (Fig. 1b). In Eqns (11), we use the coupling constant

$$H = H'_f - H'_{sc} - i(H''_f + H''_{sc}) = H' - iH'', \quad (12)$$

$$H'_f = \frac{\pi^3 \varepsilon_0 N_0 d_p^6}{16 k_B T \lambda} \frac{[(n_b^2 - \varepsilon'_p)(\varepsilon'_p + 2n_b^2) - \varepsilon''_p(\varepsilon''_p + 3n_b^2)][(n_b^2 - \varepsilon'_p)(\varepsilon'_p + 2n_b^2) - \varepsilon''_p(\varepsilon''_p - 3n_b^2)]}{[(\varepsilon'_p + 2n_b^2)^2 + \varepsilon''^2_p]^2} n_b^3, \quad (13)$$

which comprises the contributions of the optical gradient force and light scattering, respectively:

$$H'_{sc} = \frac{\pi^6 \varepsilon_0 N_0 d_p^9}{8 k_B T \lambda^4} \frac{(n_b^2 - \varepsilon'_p)^2 + \varepsilon''^2_p}{[(\varepsilon'_p + 2n_b^2)^2 + \varepsilon''^2_p]^2} n_b^8 \varepsilon''_p, \quad (14)$$

$$H''_f = \frac{3\pi^3 \varepsilon_0 N_0 d_p^6}{8 k_B T \lambda} \frac{(\varepsilon'_p - n_b^2)(\varepsilon'_p + 2n_b^2) + \varepsilon''^2_p}{[(\varepsilon'_p + 2n_b^2)^2 + \varepsilon''^2_p]^2} n_b^5 \varepsilon''_p, \quad (15)$$

$$H''_{sc} = \frac{\pi^6 \varepsilon_0 N_0 d_p^9}{24 k_B T \lambda^4} \times \frac{[(\varepsilon'_p - n_b^2)^2 + \varepsilon''^2_p][(\varepsilon'_p - n_b^2)(\varepsilon'_p + 2n_b^2) + \varepsilon''^2_p]}{[(\varepsilon'_p + 2n_b^2)^2 + \varepsilon''^2_p]^2} n_b^6. \quad (16)$$

The equations of coupled waves (11) have obvious first integrals,

$$J_{0,\Delta} = |\boldsymbol{R}|^2 \pm |\boldsymbol{S}|^2 = J_R \pm J_S, \quad (17)$$

corresponding to the fundamental law of conservation of energy when the energy is redistributed between light waves coupled via a dynamic holographic grating. The minus and plus signs in (17) correspond to codirectional (J_0) and contradirectional (J_Δ) wave mixing, respectively.

Note that both the real part of the coupling constant, H', responsible for variations in the phases of the light waves, and its imaginary part, H'', responsible for energy exchange between the waves [24–27], are determined by the contributions of the two physical mechanisms (gradient force and light scattering) underlying two-wave mixing in nanoparticle suspensions [see (12)–(16)]. The conductivity of the nanoparticles [$\varepsilon''_p = \sigma_p/(\omega\varepsilon_0)$] at the frequency of the light wave influences the four components of the coupling constant. For nonconducting nanoparticles ($\varepsilon''_p = 0$), the real part of H is contributed only the optical gradient force, and its imaginary part, only by light scattering.

4. Energy exchange in codirectional two-wave mixing

Consider the key features of energy exchange in codirectional two-wave mixing in a nanoparticle suspension when the linear polarisation of the light waves is normal to their propagation plane, i.e. parallel to the y axis (Fig. 1a). Similar coupling geometries in various nonlinear media other than nanoparticle suspensions were considered in previous studies [24–28]. It follows from Eqns (11) that, in nanoparticle suspensions, the spatially inhomogeneous disturbance of permittivity, $\Delta\varepsilon$, is proportional to the grating amplitude ($\Delta\varepsilon \propto SR^*$) [25]. Interactions in media where $\Delta\varepsilon$ is proportional to the grating modulation depth ($\Delta\varepsilon \propto 2SR^*/J_0$) were considered by Vinetskii et al. [26, 27]. Because J_0 for codirectional propagation is invariant [see Eqns (11) and (17)], the equations of coupled waves (11) written for the geometry under consideration have solutions identical in structure to those reported earlier [25–28]. According to those results, the energy exchange efficiency is conveniently quantified by the two-beam coupling gain

$$\Gamma = \frac{1}{d}\ln\frac{J_{Sd}J_{R0}}{J_{S0}J_{Rd}},$$

where $J_{R0} = |\boldsymbol{R}_0|^2$; $J_{S0} = |\boldsymbol{S}_0|^2$; $J_{Rd} = |\boldsymbol{R}_d|^2$; $J_{Sd} = |\boldsymbol{S}_d|^2$; $\boldsymbol{S}_0$, and $\boldsymbol{R}_0$ are the electric-vector amplitudes of the light waves at $x = 0$; and $\boldsymbol{S}_d$ and $\boldsymbol{R}_d$ are those at $x = d$. In the case of two-wave mixing in colloids,

$$\Gamma = H''J_0 = H''_{\rm f}J_0 + H''_{\rm sc}J_0 = \Gamma_{\rm f} + \Gamma_{\rm sc}, \qquad (18)$$

where $\Gamma_{\rm f}$ and $\Gamma_{\rm sc}$ are the gradient force and light scattering contributions to the total energy exchange.

It follows from (15) and (16) that, for specific values of $n_{\rm b}$, $\varepsilon'_{\rm p}$ and $\varepsilon''_{\rm p}$ the direction of energy transfer from one light wave to another, determined by the sign of Γ, is independent of the relative beam intensities. The energy exchange is unidirectional like in the case of scalar two-wave mixing in photorefractive crystals [26–28]. The relationship between the gradient force and light scattering contributions to the total energy exchange between the waves strongly depends on the nanoparticle diameter. When the nanoparticle diameter $d_{f\rm s}$ meets the relation

$$d_{f\rm s} = \frac{\lambda}{\pi}\left\{\frac{9\varepsilon''_{\rm p}}{n_{\rm b}[(n_{\rm b}^2 - \varepsilon'_{\rm p})^2 + \varepsilon''^2_{\rm p}]}\right\}^{1/3}, \qquad (19)$$

these contributions are equal to one another. The contribution of the gradient force prevails for $d_{\rm p} < d_{f\rm s}$, and that of light scattering prevails for $d_{\rm p} > d_{f\rm s}$.

Note that, at a given complex permittivity of the nanoparticle material ($\varepsilon'_{\rm p}$ and $\varepsilon''_{\rm p}$), one can select a dispersion medium with a refractive index $n_{\rm b0}$ such that two-wave mixing will involve no energy exchange ($\Gamma = 0$). For nanoparticles from another material, with a refractive index $n_{\rm b}$, Γ will be positive (negative) for $n_{\rm b} > n_{\rm b0}^2$ ($n_{\rm b} < n_{\rm b0}^2$). This is illustrated in Fig. 2, which shows the calculated two-beam coupling gain Γ and its components $\Gamma_{\rm f}$ and $\Gamma_{\rm sc}$ as functions of the refractive index $n_{\rm b}$ for suspensions of magnetite (Fe_3O_4) nanoparticles. In the calculations, we used the following parameters $J_0 = 10^{11}$ V^2 m^{-2}, $\beta = J_{R0}/J_{S0} = 1000$, $N_0 = 0.45 \times 10^{20}$ m^{-3}, $d_{\rm p} = 70$ nm ($f \approx 8.1 \times 10^{-3}$), real part of the permittivity of Fe_3O_4 $\varepsilon'_{\rm p} = 2.42^2$ (from the Mineralogy Database [29]) and its imaginary part $\varepsilon''_{\rm p} = 3.083$ (evaluated from the spectral reflectivity data in the same database).

For aqueous suspensions ($n_{\rm b} = 1.33$) of Fe_3O_4 nanoparticles, the nanoparticle diameter $d_{f\rm s}$ at which the contributions of the optical gradient force and light scattering to the two-beam coupling gain are equal to one another [see (19)] is 189 nm. Therefore, when the two-wave mixing conditions in a suspension of Fe_3O_4 nanoparticles correspond to Fig. 2, the light scattering contribution to the total energy exchange between the waves is small compared to the gradient force contribution ($\Gamma_{\rm sc} \ll \Gamma_{\rm f}$). At positive values of $\Gamma(n_{\rm b})$, there is a local maximum. With increasing refractive index $n_{\rm b}$, the light scattering contribution to the two-beam coupling gain rises more rapidly than the gradient force contribution [cf. Eqns (15) and (16)]. At $n_{\rm b} \sim 4$, these contributions are comparable. At higher values of $n_{\rm b}$, the light scattering contribution to the energy exchange prevails.

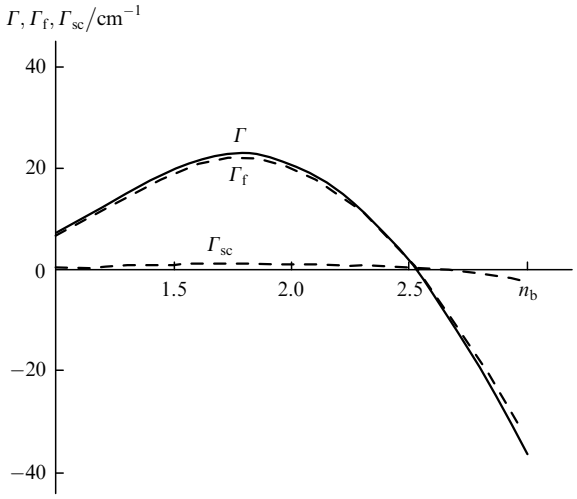

Figure 2. Calculated two-beam coupling gain Γ and its components $\Gamma_{\rm f}$ and $\Gamma_{\rm sc}$ as functions of the refractive index $n_{\rm b}$ for suspensions of Fe_3O_4 nanoparticles.

5. Energy exchange in contradirectional two-wave mixing

Consider contradirectional two-wave mixing in a nanoparticle suspension when the linear polarisation of the light waves is normal to their propagation plane, i.e. parallel to the y axis (Fig. 1b). In contrast to codirectional two-wave mixing, where the sum J_0 is constant, contradirectional mixing is characterised by a constant value of the difference J_Δ [see Eqns (11) and (17)]. Therefore, the equations obtained by Vinetskii et al. [28] for contradirectional two-wave mixing in media with spatially inhomogeneous disturbances $\Delta\varepsilon \propto 2SR^*/J_0$ have solutions different from those to the equations for coupled waves in media with disturbances $\Delta\varepsilon \propto SR^*$. Note that, as pointed out by Yeh [30], the sum intensity is noninvariant ($J_0 \neq$ const) in the case of contradirectional wave mixing, which makes it impossible to obtain a close-form solution of the vector equations for coupled waves.

The solution to Eqns (11) in the case of contradirectional wave mixing can be found in the same manner as the

solution to the equations for codirectional wave mixing [25–28]. From Eqns (11) one can obtain nonlinear equations in $J_R = |\boldsymbol{R}|^2$ and $J_S = |\boldsymbol{S}|^2$. Integration of these equations using the invariant J_Δ [see Eqn (17)] gives

$$J_S(x) = \frac{J_\Delta}{(J_\Delta J_{Sd}^{-1} + 1)\exp[H'' J_\Delta (x-d)] - 1}, \qquad J_R(x) = \frac{J_\Delta}{(J_\Delta J_{R0}^{-1} - 1)\exp(-H'' J_\Delta x) + 1}. \tag{20}$$

J_Δ can be determined by numerically solving the equation

$$\frac{J_{R0} - J_\Delta}{J_{R0}} \frac{J_{Sd} + J_\Delta}{J_{Sd}} = \exp(H'' J_\Delta d), \tag{21}$$

which follows from (20) with the boundary conditions $J_R(0) = J_{R0}$ and $J_S(d) = J_{Sd}$.

Equation (21) allows us to introduce in the case of contradirectional wave mixing the coefficient

$$\Gamma_1 = \frac{1}{d} \ln \frac{J_{Rd} J_{S0}}{J_{R0} J_{Sd}} = H'' J_\Delta \tag{22}$$

analogous to the two-beam coupling gain for codirectional wave mixing [see Eqn (18)] introduced in previous studies [25–28].

The coefficient Γ_1, defined by (22) for codirectional wave mixing, differs from the two-beam coupling gain

$$\Gamma_2 = \frac{1}{d} \ln \left(\frac{J_{S0} J_{R0}}{J_{Sd} J_{Rd}} \right)$$

introduced by Vinetskii et al. [28] for this type of coupling in photorefractive crystals, which have inhomogeneous disturbances of their permittivity, $\Delta\varepsilon \propto 2SR^*/J_0$. In such media, Γ_2 is proportional to the coupling coefficient from the equations for coupled waves. In media with $\Delta\varepsilon \propto SR^*$, which include the colloids under consideration, Γ_2 is a more intricate function of H'' than is the coefficient defined by (22).

Note that, in the case of codirectional propagation, Γ is independent of the coupling length d [see Eqn (18)]. In contradirectional wave mixing, Γ_1 is a function of d because the invariant J_Δ depends on the hologram thickness [see Eqns (21) and (22)]. At a small coupling length ($d \to 0$), the intensity of the light waves varies insignificantly, and Γ_1 is at its maximum, equal approximately to $H''(J_{R0} - J_{Sd})$. For $\beta = J_{R0}/J_{Sd} \gg 1$, the weaker wave is amplified exponentially over the coupling length: $J_{S0} \approx J_{Sd} \exp(H'' J_{R0} d)$. When the coupling length is large, an inversion occurs: $J_{R0} \approx J_{S0}$ and $J_{Rd} \approx J_{Sd}$. Therefore, $J_\Delta \approx 0$ ($\Gamma_1 \approx 0$), which corresponds to saturation of the energy exchange between the waves at sufficiently large d. Figure 3 shows the calculated two-beam coupling gain Γ_1, J_{S0}, J_{Rd} as functions of d at $\lambda = 640$ nm for suspensions of Fe_3O_4 nanoparticles. These data illustrate the above features of energy exchange in contradirectional wave mixing. In the calculations, the nanoparticle concentration was taken to be $N_0 = 10^{20}$ m^{-3}, and the refractive index of the dispersion medium was set to be equal to that of water, $n_b = 1.33$. The other parameters were the same as those for the curves in Fig. 2.

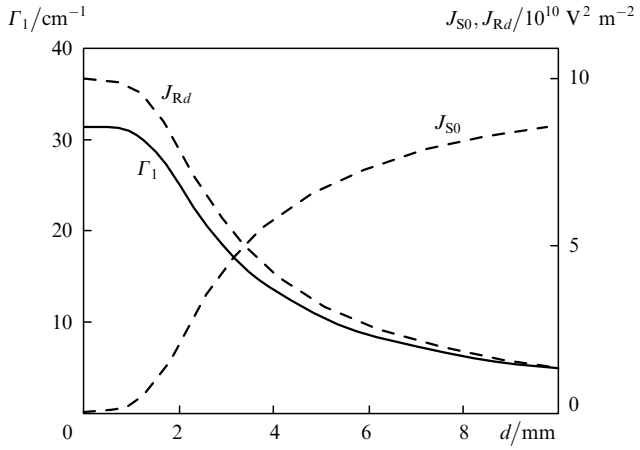

Figure 3. Calculated two-beam coupling gain Γ_1, J_{S0} and J_{Rd} as functions of hologram thickness d in aqueous suspensions ($n_b = 1.33$) of Fe_3O nanoparticles.

6. Dynamic-grating amplitude for different types of coupling

Two-wave mixing in suspensions of conducting nanoparticles leads to the formation of a dynamic permittivity grating: $\Delta\varepsilon = (\Delta\varepsilon_1/2)\exp(i\boldsymbol{Kr}) + \text{c.c.}$ In the case of codirectional propagation, considered in Section 4, the small contribution of light scattering can be neglected, and the grating amplitude $\Delta\varepsilon_{1t}$ in a nanoparticle suspension can be represented in the form

$$\Delta\varepsilon_{1t} = \frac{GJ_0 \exp\{i[\phi_{S0} - \phi_{R0} - \phi_\delta - (H'_f J_0 x/2)]\}}{[\beta^{-1}\exp(H''_f J_0 x) + \beta\exp(-H''_f J_0 x) + 2]^{1/2}}, \tag{23}$$

where ϕ_{S0} and ϕ_{R0} are the initial phases of the signal and reference beams, respectively, at $x = 0$,

$$G = \frac{\varepsilon_0 \pi^2 d_p^6 n_b^4 N_0}{16 k_B T} \frac{(\varepsilon'^2_p - n_b^2)^2 + \varepsilon''^2_p}{(\varepsilon'^2_p + 2n_b^2)^2 + \varepsilon''^2_p}, \tag{24}$$

$$\phi_\delta = 2\arctan\left[\frac{3n_b^2 \varepsilon''_p}{(\varepsilon'_p + 2n_b^2)(\varepsilon'_p - n_b^2) + \varepsilon''^2_p}\right]. \tag{25}$$

In the case of contradirectional propagation, considered in section 5, with the light scattering contribution neglected, the grating amplitude $\Delta\varepsilon_{1r}$ in a nanoparticle suspension has the form

$$\Delta\varepsilon_{1r} = \frac{GJ_\Delta \exp\{i[\phi_{Sd} - \phi_{R0} - \phi_\delta + \Delta\phi(x)]\}}{\{[1 + (J_\Delta/J_{Sd})]\exp[H''_f J_\Delta (x-d)] + [1 - (J_\Delta/J_{R0})]\exp(-H''_f J_\Delta x) - 2\}^{1/2}}, \tag{26}$$

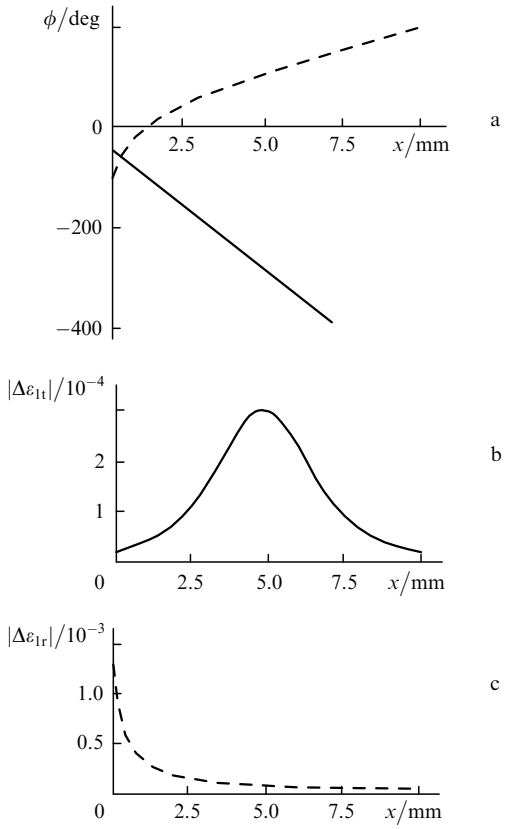

Figure 4. Phase ϕ (a) and amplitudes $|\Delta\varepsilon_{1t}|$ (b) and and $|\Delta\varepsilon_{1r}|$ (c) of 10-mm-thick permittivity gratings in aqueous suspensions of Fe_3O_4 nanoparticles for codirectional (solid curves) and contradirectional (dashed curves) two-wave mixing.

where the phase advance due to wave mixing is

$$\Delta\phi(x) = \frac{H'_f}{2H''_f} \times \ln\left\{\frac{\exp[H''_f J_\Delta (x-d)](J_\Delta + J_{Sd}) - J_{Sd}}{\exp(-H''_f J_\Delta x)(J_\Delta - J_{R0}) + J_{R0}}\right\} + \frac{H'_f J_\Delta d}{2}. \quad (27)$$

In codirectional wave mixing, the phase advance ϕ of the $\Delta\varepsilon$ grating is linear with the longitudinal coordinate x [see Eqn (23)] and is proportional to the real part of the coupling constant H'_f [see Eqn (13)]. For contradirectional propagation, the phase ϕ of the grating is a nonlinear function of x [see Eqns (26) and (27)] and depends on both the real (H'_f) and imaginary (H''_f) parts of the coupling constant [see Eqn (15)]. Figure 4a shows the calculated phase ϕ of the grating as a function of x for codirectional and contradirectional two-wave mixing at 640 nm in suspensions of magnetite (Fe_3O_4) nanoparticles. In the calculations, the nanoparticle concentration was taken to be $N_0 = 0.45\times 10^{20}$ m^{-3} for codirectional propagation and 10^{20} m^{-3} for contradirectional propagation. In both cases, the refractive index of the dispersion medium was $n_b = 1.33$, the hologram thickness was $d = 10$ mm, and the phases of the light waves were $\phi_{Sd} = \phi_{S0} = \phi_{R0} = 0$. The other parameters were the same as those for the curves in Figs 2 and 3. Note that, in the case of codirectional propagation, the linear phase advance of the grating leads to a tilt of its isopleths with respect to the x axis, which corresponds to a transverse displacement (along the z axis) of the $\Delta\varepsilon$ grating relative to the initial interference pattern with a period Λ by $\Delta z(x) = \Lambda[(H'_f J_0 x/2) + \phi_\delta]/(2\pi)$. In the case of contradirectional propagation, the nonlinear phase advance of the grating leads to a continuous displacement of the hologram along the x axis relative to the initial interference pattern.

Figures 4b and 4c show the dependences of the permittivity grating amplitude $\Delta\varepsilon_{1t,1r}$ on $\phi(x)$ in Fe_3O_4 nanoparticle suspensions for codirectional and contradirectional propagation, respectively (corresponding to the $\phi(x)$ curves in Fig. 4a). In the case of codirectional propagation, $|\Delta\varepsilon_{1t}(x)|$ has a maximum at the point x_{max} where J_S and J_R are equal to one another and the magnitudes of their gradients, dJ_S/dx and dJ_R/dx, are maximal [25]. In the case of contradirectional propagation, $|\Delta\varepsilon_{1r}(x)|$ reaches a maximum at the boundary $x = 0$, where J_S and J_R are maximal.

It follows from Fig. 2 and relation (18) that, in the case of two-wave mixing in an Fe_3O_4 nanoparticle suspension with a refractive index of the dispersion medium $n_{b0} = 2.52$, the imaginary part of the coupling constant is $H'' \approx H''_f = 0$. Therefore, there is no energy exchange between the light waves, and the amplitudes of the dynamic gratings produced in the colloid are independent of $|\Delta\varepsilon_{1t,1r}| = \text{const}$ [see Eqns (23) and (26)]. In the case of codirectional propagation with $H'' \approx H''_f = 0$, the phase advance along the x axis is linear, in contrast to the case $H''_f \neq 0$ [see Eqn (27)].

7. Conclusions

Mixing of two monochromatic light waves in a nanoparticle suspension leads to the formation of a dynamic permittivity grating and energy exchange between the waves. The optical nonlinearity underlying such coupling is due to the optical gradient force acting on the nanoparticles, which produces a spatially inhomogeneous nanoparticle distribution in the colloid. This leads to inhomogeneous disturbances of the permittivity of the medium and inhomogeneous light scattering, which in turn influence the optical field.

In the general case, the permittivity grating resulting from two-wave mixing in a suspension of spherical nanoparticles comprises local and nonlocal components. The latter is due to light absorption and scattering by the nanoparticles. Two-wave mixing via the nonlocal component of the dynamic grating in a suspension of magnetite (Fe_3O_4) nanoparticles leads to efficient energy exchange between the waves. When the nanoparticle diameter is within 10 nm, the major contribution to the coupling comes from the gradient mechanism of optical nonlinearity.

The direction of energy exchange between the waves is independent of their relative intensities and, at a given permittivity of the nanoparticles, it is determined by the refractive index of the dispersion medium, n_b. One can select a dispersion medium with a refractive index n_{b0} such that there will be no energy exchange between the waves. This refractive index is close to that of the nanoparticles. In two-wave mixing, the direction of energy transfer in colloids with $n_b > n_{b0}$ is opposite to that in colloids with $n_b < n_{b0}$.

In the case of two-wave mixing in a suspension of nonconducting nanoparticles, the nonlocal component of the dynamic grating is negligible, there is no energy exchange between the waves, and the coupling via the local component leads only to changes in the phases of the light waves.

Acknowledgements. This work was supported in part by the Russian Foundation for Basic Research (Grant No. 08-02-99025-r_ofi).

References

1. Mikheeva O.P., Sidorov A.I. *Zh. Tekh. Fiz.*, **74**, 77 (2004).
2. Karavanskii V.A., Simakin A.V., Krasovskii V.I., Ivanchenko P.V. *Kvantovaya Elektron.*, **34**, 644 (2004) [*Quantum Electron.*, **34**, 644 (2004)].
3. Kulchin Yu.N., Shcherbakov A.V., Dzyuba V.P., Voznesenskii S.S., Mikaelyan G.T. *Kvantovaya Elektron.*, **38**, 154 (2008) [*Quantum Electron.*, **38**, 154 (2008)].
4. Falcão-Filho E.L., de Araujo Cid B., Rodrigues J.J. Jr. *J. Opt. Soc. Am. B*, **24**, 2948 (2007).
5. López-Mariscal C., Gutiérrez-Vega J., McGloin D., Dholakia K. *Opt. Express*, **15**, 6330 (2007).
6. Matuszewski M., Krolikowski W., Kivshar Y.S. *Opt. Express*, **16**, 1371 (2008).
7. El-Ganainy R., Christodoulides D.N., Rotschild C., Segev M. *Opt. Express*, **15**, 10207 (2007).
8. Pilipetskii N.F., Rustamov A.R. *Pis'ma Zh. Eksp. Teor. Fiz.*, **2**, 88 (1965).
9. Zakharov V.E., Shabat A.B. *Zh. Eksp. Teor. Fiz.*, **61**, 119 (1971).
10. Shen Y.R. *The Principles of Nonlinear Optics* (New York: Wiley, 1984; Moscow: Nauka, 1989).
11. Ashkin A. *Phys. Rev. Lett.*, **24**, 156 (1970).
12. Ashkin A., Dziedzic J.M. *Appl. Phys. Lett.*, **19**, 283 (1971).
13. Gordon J.P. *Phys. Rev. A*, **8**, 14 (1973).
14. Burns M.M., Fournier J.-M., Golovchenko J.A. *Phys. Rev. Lett.*, **63**, 1233 (1989).
15. Tamm I.E. *Osnovy teorii elektrichestva* (Fundamentals of the Theory of Electricity) (Moscow: Nauka, 1989).
16. Garnett J.M.C. *Philos. Trans. R. Soc. London*, **203**, 385 (1904).
17. Garnett J.M.C. *Philos. Trans. R. Soc. London*, **205**, 237 (1906).
18. Mishchenko M.I., Trvis L.D., Lacis A.A. *Scattering, Absorption and Emission of Light by Small Particles* (Cambridge: Cambridge Univ. Press, 2004).
19. Bohren C.F., Huffman D.R. *Absorption and Scattering of Light by Small Particles* (New York: Wiley, 1983; Moscow: Mir, 1986).
20. Van de Hulst H.C. *Light Scattering by Small Particles* (New York: Wiley, 1957; Moscow: Inostrannaya Literatura, 1961).
21. Loitsyanskii L.G. *Mekhanika zhidkosti i gaza* (Fluid Mechanics) (Moscow: Nauka, 1987).
22. Lightfoot E.N. *Transport Phenomena and Living Systems: Biomedical Aspects of Momentum and Mass Transport* (New York: Wiley, 1974; Moscow: Mir, 1977).
23. Karpov S.V., Kodirov M.K., Ryasnyansky A.I., Slabko V.V. *Kvantovaya Elektron.*, **31**, 904 (2001) [*Quantum Electron.*, **31**, 904 (2001)].
24. Chaban A.A. *Zh. Eksp. Teor. Fiz.*, **57**, 1388 (1969).
25. Stasel'ko D.I., Sidorovich V.G. *Zh. Tekh. Fiz.*, **44**, 580 (1974).
26. Vinetskii V.L., Kukhtarev N.V., Markov V.B., Odulov S.G., Soskin M.S. *Izv. Akad. Nauk SSSR, Ser. Fiz.*, **41**, 812 (1977).
27. Vinetskii V.L., Kukhtarev N.V., Odulov S.G., Soskin M.S. *Usp. Fiz. Nauk*, **129**, 113 (1979).
28. Vinetskii V.L., Kukhtarev N.V. *Kvantovaya Elektron.*, **5**, 405 (1978) [*Sov. J. Quantum Electron.*, **8**, 231 (1978)].
29. http://www.webmineral.com/data/Magnetite.shtml.
30. Yeh P. *J. Opt. Soc. Am. B*, **4**, 1382 (1987).